Pis'ma v ZhETF, vol. 77, iss. 4, pp. 202 – 207 © 2003 February 25

Many particle interaction in tunneling spectroscopy of impurity states on the InAs(110) surface

P. I. Arseev[1)], *N. S. Maslova*[+], *V. I. Panov*[+], *S. V. Savinov*[+], *C. Van Haesendock*[*]

Lebedev Physical Institute RAS, 117924 Moscow, Russia

[+]*Department of Physics, Moscow State University, 119899 Moscow, Russia*

[*]*Laboratorium voor Vaste-Stof Fysica en Magnetisme, Katholieke Universiteit Leuven, B-3001 Leuven, Belgium*

Submitted 17 December 2002

We report on the direct observation by low temperature scanning tunneling microscopy and scanning tunneling spectroscopy of the *d*-orbitals of a Mn *p*-type impurity appearing on a cleaved InAs(11O) surface. We show that the crucial interplay between non-equilibrium charging effects and many particle interaction leading to Coulomb singularities provides a consistent description of the experimental results.

PACS: 73.20.–r, 73.40.Gk

The invention of scanning tunneling microscopy (STM) and spectroscopy (STS) was expected to provide a reliable tool to determine the local surface electronic structure with a spatial resolution comparable to the interatomic distance. For several surfaces STM and STS measurements indeed provided crucial information about the local electronic density of states, e.g., in the case of the Si (7×7) reconstruction [1]. For other surfaces, however, discussions are still going on about the unusual tunneling characteristics which are observed. For these surfaces more experimental data as well as an improved understanding of nanometer scale tunneling phenomena are clearly needed [2]. In particular, this applies to low temperature STM and STS measurements because of the possible presence of a nonequilibrium electron distribution in the tunnel contact area, a strong modification of the initial electronic spectrum due to tip-sample interactions, and many particle correlation effects [3]. The qualitative changes in understanding of tunneling phenomena in STM/STS experiments revealed the sighnificant importance of relaxation processes and nonequilibrium interaction effects in behaviour of tunneling characteristics ultra small junctions. Now it is clear that non-equilibrium electron distribution in the tunneling contact area and interaction between tunneling particles give rise to strong modification of initial local density of states and tunneling conductivity spectra. Moreover, tunneling amplitude itself be also altered by Coulomb interaction of conduction electrons in metallic tip with nonequilibrium charges localised at the impurity states. In this case Coulomb singularity in tunneling current near the threshold value of bias voltage can be observed in STM/STS experiments. In the present paper we show that crucial interplay between the effects connected with changes of initial density of states due to nonequilibrium charge distribution and the effects assosiated with modification of tunneling amplitude due to many-particle Coulomb interaction can result in new unusual features in tunneling characteristics

Here, we present the results of low temperature STM and STS measurements on Mn doped InAs single crystal surfaces which are obtained by in-situ cleavage of single crystals along the (110) plane. There exists a significant difference in the local electronic properties of narrow and wide band gap III-V compound semiconductors [4]. Narrow band gap materials such as InAs have been less intensively investigated when compared to the wide band gap ones such as GaAs. We therefore decided to perform a more detailed study of the behavior of individual dopant atoms on an InAs surface. In the STM as well as in the STS based images we observed a remarkable cross-like feature within a particular range of voltages applied between the sample and the STM tip. A similar structure was recently observed with low temperature STM and STS for a Cr(001) surface and was explained in terms of an orbital Kondo resonance in the Cr [5]. We show that the physical process causing the formation of the cross-like surface structures in our semiconducting samples is very different from the mechanism which was proposed to explain the appearance of the cross-like features in a transition metal.

Our STM and STS data have been obtained with a home built low temperature microscope with an in-situ

[1)]e-mail: ars@lpi.ru

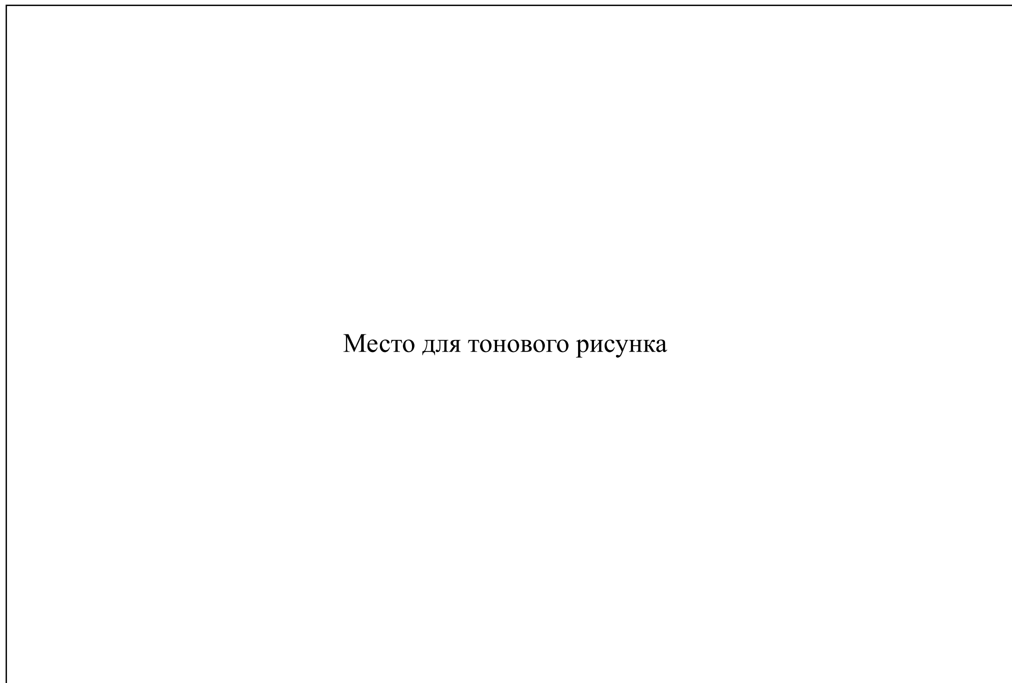

Fig.1. Low temerature STM images of a Mn dopant atom on the InAs(110) surface obtained at different values of the applied sample bias voltage: (a) $V = -0.5$ V, (b) $V = -0.7$ V, (c) $V = -1$ V, (d) $V = 0.5$ V, (e) $V = 0.7$ V. In (f) we show a topographic image at $V = -0.5$ V during STS measurements. The white arrow in (d) indicates the stripe where we have collected the STS data for the 1D cross section shown in Fig.3

sample cleavage mechanism. The microscope operates at liquid helium temperature and in the presence of magnetic fields up to 7 T [6]. The scanning of the STM tip (PtIr wire cut with scissors) is controlled by commercially available control electronics (Omicron Gmbh). The samples are p-type InAs single crystals doped with Mn atoms. The concentration of dopant atoms is relatively high and is about $5 \cdot 10^{17}$cm^{-3}. Mn atoms are known to act as acceptors in InAs where they are included as substitutional atoms occupying the In sublattice. The samples are cleaved along the (110) natural cleavage plane after the temperature of the system has reached 4.5 K. The residual partial pressure for all gases, in partiular for oxygen, is very low, implying that the cleaved surfaces remain atomically clean for about two weeks.

The STM/STS measurements presented below are obtained in two different modes of operation. The first mode is the usual constant current mode STM, while the second mode is the current imaging tunneling spectroscopy (CITS) mode which is derived from the STS measurements. In the CITS mode the STM tip is scanning a grid (typically 40×40 points) and at every point of the grid the feedback loop is interrupted for some time, allowing to measure the current-voltage characteristic for this point. Next, the feedback is restored and the tip is moved to the next point of the grid. Therefore, one obtains the following experimental data set: a 2D array of points containing topographic information, and a 2D array of data files containing the local $I(V)$ curves. Previous investigations have focused on the best way to interpret the second "spectroscopic" data set. The most commonly used measure of the local density of states is the normalized conductivity $(dI/dV)/(I/V)$ [7].

Because of the digital method used for calculating the derivative dI/dV and because of the normalization, spatial averaging of the spectroscopic data is required to obtain an acceptable signal to noise ratio. This is achieved by calculating average $I(V)$ curves, where the average includes the point of the grid as well as the surrounding points, implying that the spatial resolution is somewhat reduced. After this averaging procedure, it is possible to "slice" the 2D array of averaged $I(V)$ curves at specific values of the applied bias voltage, resulting in a 2D distribution of the tunneling current for the grid. In a similar way one can calculate the average normalized conductivity for every point of the grid, and again one can "slice" the grid of normalized conductivity data at specific values of the applied bias voltage, resulting in a 2D array of normalized and averaged data. A simi-

Место для тонового рисунка

Fig.2. Voltage dependence of the normalized tunneling conductivity $(dI/dV)(I/V)$ averaged over the whole surface area corresponding to the STM images shown in Fig. 1. The insets (a)–(g) correspond to 2D "slices" of the normalized tunneling conductivity data at different vaues of the bias voltage. The bias voltage used for the slicing is marked by the arrows. The insets (a1)–(g1) correspond to 2D "slices" of the $I(V)$ data. The images based on the $I(V)$ data have been placed above the corresponding images obtained from the differential conductivity data

lar procedure can also be used for a linear cross-section of an STM image (1D array of normalized conductivity data). As we will explain in more detail below, the complexity of both the experimental data and the physical processes occurring in nanometer scale junctions, different ways of representing the data are required to draw reliable conclusions.

In Fig.1 we show the results of topographical STM measurements on surface area 6×6 nm in the vicinity of a Mn dopant atom at different values of the applied bias voltage. For negative voltages, we observe a remarkable cross-like feature protruding from the atomic lattice background around the impurity atom: -0.5 V (Fig.1a), -0.7 V (Fig.1b) and -1 V (Fig.1c). The brightness of the cross-like feature decreases when increasing the bias voltage. At positive sample bias voltage a more spherical depression is observed around the impurity atom, and the depression becomes more localized when increasing

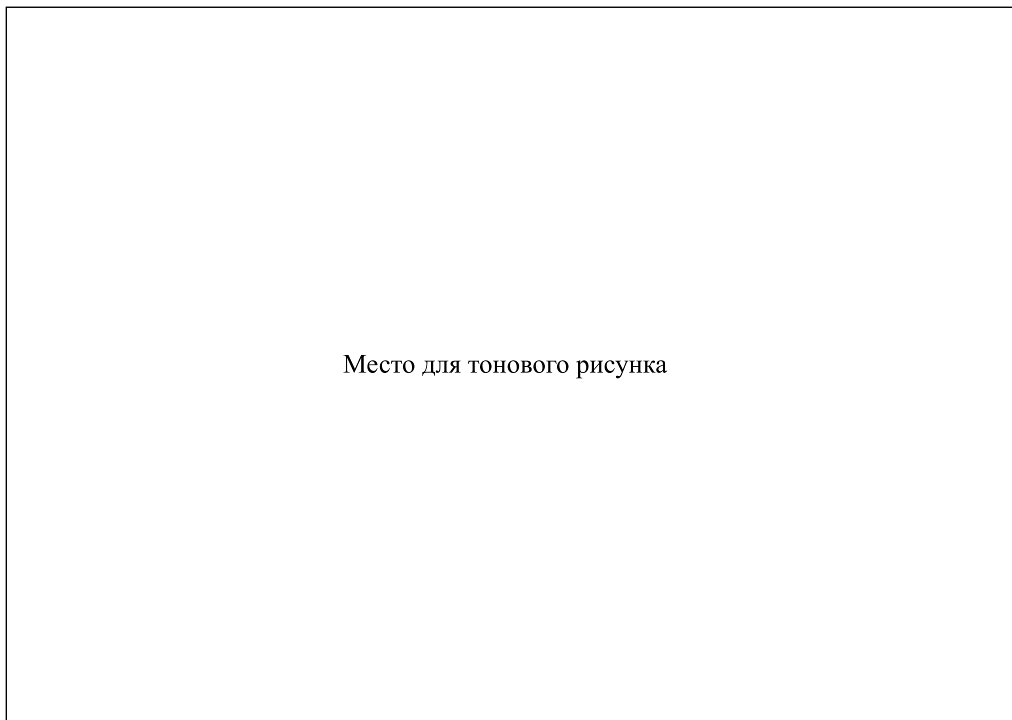

Fig.3. Quasi 1D "cross-section" of the normalized tunneling conductivity $(dI/dV)(I/V)$ averaged along the width of the stripe indicated by the arrow in Fig.1d

the bias voltage: 0.5 V (Fig.1d), 0.7 V (Fig.1e). In order to illustrate the good quality of our STS measurements which are discussed in more detail below, we show in Fig.1f shows the STM topography which is obtained from the STS data. The image corresponds to a 2D grid with 40×40 current values measured at $V = -0.5$ V. Atomic details as well as the cross-like feature around the impurity atom can clearly be observed.

In Fig.2 we plot the normalized voltage dependence of the differential conductivity. This result has been averaged over the 40×40 points of the 2D grid (see Fig.1f). The images which have been inserted in Fig.2 correspond to 2D "slices" of the normalized tunneling conductivity at the bias voltages indicated by the arrows (Fig.2a–g). In order to stress the difference between the information contained in the normalized conductivity data and in the original $I(V)$ curves, we have added to Fig.2 "slices" of the $I(V)$ data for different bias voltages Fig.2a1–g1. For positive voltages the feature around the Mn dopant atom appears as a protrusion in the images based on the normalized conductivity, while the feature appears as a depression in the images based on the $I(V)$ data.

Next, we come to the physical origin of the bright cross-like feature which is the key result of our present STM and STS investigation. For negative polarity of the sample voltage we observe a bright cross-like feature when $-1\,\mathrm{V} < V < -0.5\,\mathrm{V}$ which corresponds to the electron density of the Mn acceptor d-orbital state hybridized with the InAs lattice states in the valence band (Fig.2a-c). For small bias voltages the Mn impurity d-orbital state is close to be singly occupied. When the value of the applied voltage approaches the acceptor energy level ϵ one expects an enhanced tunneling conductivity in the voltage range $|eV - \varepsilon_d| < \Gamma$ when moving the STM tip in the vicinity of the Mn atom. The parameter Γ corresponds to the lifetime broadening of the energy level ε due to the coupling with the semiconductor valence band states. The enhanced tunneling current and local tunneling conductivity near the Mn impurity therefore result from the increased semiconductor local density of states formed in the vicinity of a a Mn impurity. This density of states directly reflects the non-spherical symmetry of the localized Mn impurity d-level.

Another factor causing an enhanced tunneling current and conductivity may be related to the non-equilibrium many particle Coulomb interactions in the nanoscale tunneling contact. The many particle Coulomb interaction of the conduction electrons residing at the STM tip apex with the positively charged impurity state is expected to result in a power law sin-

gularity of the tunneling current and conductivity near a threshold value of the applied bias voltage [3]. When the tunneling rate Γ_t from the the STM tip into the localized impurity state strongly exceeds the electron transition rate Γ due to the coupling of the d-orbital state to the semiconductor continuum states, a non-equilibrium positive charge will start to build up near the impurity atom when the negative applied bias is close to the threshold value $|eV - \varepsilon| < \Gamma$.

The Coulomb interaction between the positively charged impurity with the conduction electrons gives rise to a power law dependence of the $I(V)$ characteristic with a negative power law exponent $a = W\nu$, where W is the averaged value of the impurity Coulomb potential and ν is the electron density of states for the metallic tip [3].

$$I(V) = \frac{\gamma_t}{2W\nu}\left[\frac{D^2}{(eV-\varepsilon_d)^2+(\gamma_t+\gamma)^2}\right]^{W\nu}\sin(2W\nu\phi)\,, \quad (1)$$

where $\phi = arcctg(\frac{eV-\varepsilon_d}{\gamma+\gamma_t})$. Therefore, one expects an additional enhancement of the tunneling current near the impurity atom when the applied voltage approaches its threshold value. For bias voltages $-0.5\,\mathrm{V} < V < 0.5\,\mathrm{V}$ the bright cross-like feature becomes smeared out and the spatial structure of the local density of states is no longer visible in the images obtained from the STS data.

In Fig.2 a strongly enhanced tunneling conductivity is observed in the vicinity of the impurity atom when the applied bias voltage approaches the conduction band edge. Such a behavior of the local tunneling conductivity is consistent with non-equilibrium charging effects [8]. The position of the impurity energy level depends on the electron filling numbers because of the on-site Coulomb interaction between electrons of opposite spins that are localized on the impurity. When varying the applied bias voltage and the tunneling current, one can vary the filling numbers for the localized electrons and hence shift the value of the impurity energy level. This mechanism is expected to become very effective near the band gap edges, resulting in considerable changes of the tunneling current when varying the bias voltage. As shown in more detail in [8], the dependence of the impurity energy on the electron filling numbers induces a non-monotonic behavior of the tunneling conductivity. Electron scattering by the impurity potential causes the appearance of localized states near the band gap edges in the surface electronic structure. For a positively charged impurity this split state might be slightly below the bottom of the conduction band and for a negatively charged impurity the split state may be slightly above the valence band edge.

It is clear that the peak in the tunneling conductivity near the conduction band edge can not be associated with a Kondo effect. In contrast to the experimental observations reported in [5], no specific features can be observed near the Fermi level, i.e., for bias voltages smaller than 100 meV. In the case of a Kondo resonance, an asymmetric shape of the tunneling conductivity can occur due to Fano interference effects. For a Fano resonance the shift of the peak in the tunneling conductivity is determined by the total impurity level width Γ which hardly exceeds 100 meV. In the present experiment the peak in the tunneling conductivity spectra appears for a bias voltage of 400 meV, and can not be explained in terms of a Kondo resonance even when invoking the presence of Fano interference effects. For our experiments we have to connect the tunneling conductivity peak to a localized state split from the conduction band due to electron scattering by the impurity potential.

For bias voltages $1\,\mathrm{V} < V < 1.5\,\mathrm{V}$ the bright cross-like feature is clearly present in the spatial distribution of the local tunneling conductivity around the impurity atom. On the other hand, we note the remarkable fact that in the spatial distribution of the tunneling current the impurity atom appears as a dark cross, corresponding to a locally reduced tunneling current. Such a unusual behavior of the tunneling characteristics can be accounted for by the many particle non-equilibrium Coulomb interaction of a negatively charged impurity with the Fermi sea of the conduction electrons in the STM tip. When the tunneling rate Γ_t from the STM tip into the localized impurity state strongly exceeds the electron transition rate Γ for the semiconductor continuum states, a non-equilibrium negative charge appears near the impurity atom for negative tip voltages which are close to the threshold value $|eV - \varepsilon - U| < \Gamma$ with U the on-site Coulomb repulsion between localized electrons. Near the negatively (positively) charged impurity one expects the existence of an area with a decreased (increased) density of states deep in the continuum states (conduction and valence bands, respectively). This area with a modified density of states has a size of the order of the Debye screening radius. Consequently, the tunneling current becomes suppressed near the impurity atom when compared to a defect free surface area.

An essential feature of our theoretical model is that due to the many particle interaction effects the *tunneling current* is expected to reveal a power law singularity with a positive exponent $a = W\nu$ [8].

$$I(V) = \frac{\gamma_t}{2W\nu}\times$$
$$\times\left[\frac{(eV-\varepsilon_d-U)^2+(\gamma_t+\gamma)^2}{D^2}\right]^{W\nu}\sin(2W\nu\phi)\,, \quad (2)$$

where $\phi = arcctg(\frac{eV-\varepsilon_d-U}{\gamma+\gamma_t})$. On the other hand, this power law singularity can be reflected as an effective enhancement of the *normalized tunneling conductivity* for the same range of bias voltages if power law exponent satisfies the condition $0 < W\nu < 0.5$. In this case the singularity exceeds the decrease of semiconductor density of states within the considered range of bias voltages.

$$(dI/dV) = \frac{\gamma_t(eV-\varepsilon_d-U)}{D^2} \times \times \left[\frac{D^2}{(eV-\varepsilon_d-U)^2+(\gamma_t+\gamma)^2}\right]^{1-W\nu} \sin(2W\nu\phi) \,. \quad (3)$$

For $(eV - \varepsilon_d - U)$ $\gamma_t + \gamma$ and rather small values of $\gamma_t + \gamma$ tunneling conductivity strongly increases. In this case the singularity exceeds the decrease of semiconductor density of states within the considered range of bias voltages. Finally, we want to point out that for our STS measurements we are dealing with semiconductor density of states in the conduction and valence band which are strongly modified by the presence of the impurity atom due to the appearance of non-equilibrium impurity charges and many particle Coulomb interaction effects between the tunneling electrons and the charged impurity. In Fig.3 we show a 1D cross-section of the normalized conductivity along the direction indicated by the arrow in Fig.1d. The most intriguing feature of the 1D cross-section is the remarkable enhancement of the normalized differential conductivity inside the conduction and valence bands near the impurity atoms, with almost no visible variations inside the band-gap while changing the distance from the impurity. As explained above, this may be linked to the interplay between a many particle Coulomb singularity and a modification of the non-perturbed semiconductor density of states by tunneling in the presence of a charged impurity.

In conclusion, we reported on the direct observation by low temperature STM and STS measurements of the *d*-orbitals of a Mn *p*-type impurity appearing on a cleaved InAs(110) surface. The remarkable cross-like shape of the STM image of the impurity as well a the shape of the differential tunneling conductivity can not be explained in terms of a Kondo resonance. Non-equilibrium charge interaction effects provide a consistent description of our experimental results.

This work was supported by the Russian Foundation for Basic Research (projects # 02-02-17361, # 00-15-96555 and # 00-02-17759) and by the Physics of Solid State Nanostructures (project 7) and Surface Atomic Structures (project 1.2) programs. Additonal support has been obtained from the Fund for Scientific Research – Flanders (Belgium) as well as from the Belgian Interuniversity Attraction Poles (IAP) and the Flemish Concerted Action (GOA) research programs.

---

1. G. Binnig, H. Rohrer, and E. Weibel, Phys. Rev. Lett **50**, 120 (1983).
2. A. Depuydt, C. Van Haesendonck, N.S. Maslova et al., Phys. Rev. **B60**, 2619 (1999).
3. P.I. Arseev, N.S. Maslova, V.I. Panov, and S.V. Savinov, JETP Lett. **76**, 287 (2002).
4. R.M. Feenstra, Phys. Rev **B50**, 4561 (1994).
5. O.Yu. Kolesnychenko, R. de Kort, M.I. Katsnelson et al., Nature **415**, 507 (2002).
6. S.I. Vasil'ev, S.I. Oreshkin, S.V. Savinov et al., Instrum. Exp. Tech **40**, 566 (1997).
7. J.A. Stroscio, R.M. Feenstra, and A.P. Fein, Surf. Sci. **181**, 295 (1987).
8. P.I. Arseev, N.S. Maslova, and S.V. Savinov, JETP Lett. **68**, 320 (1998).